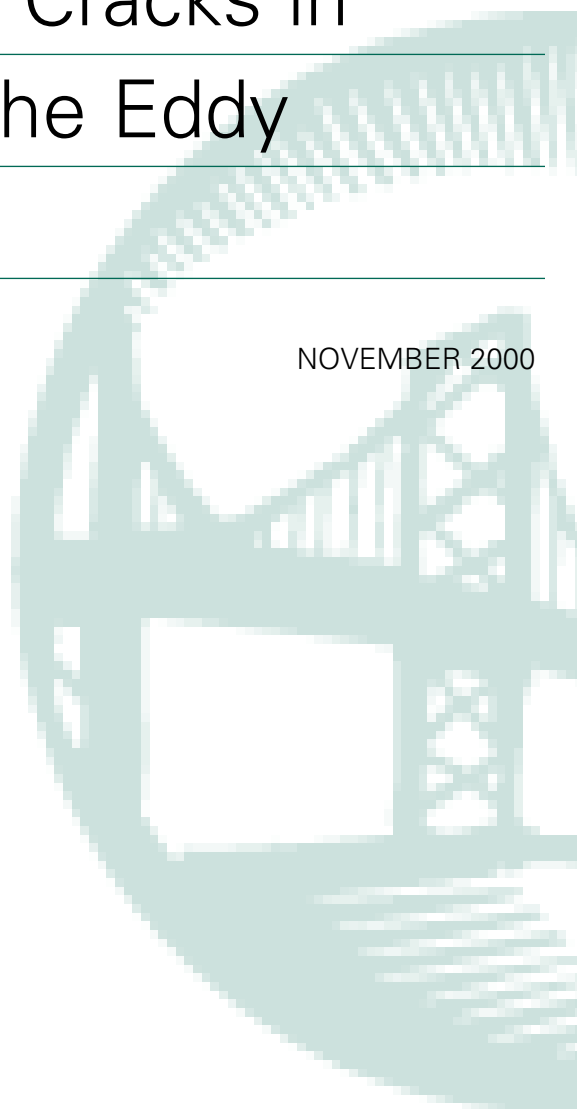


# Detection and Sizing of Cracks in Structural Steel Using the Eddy Current Method

FHWA-RD-00-018

NOVEMBER 2000



U.S. Department of Transportation  
**Federal Highway Administration**

Research, Development, and Technology  
Turner-Fairbank Highway Research Center  
6300 Georgetown Pike  
McLean, VA 22101-2296

## FOREWORD

This report documents the findings of research related to the application of the Eddy Current method for crack detection in structural steel members of highway bridges. Historically, the Eddy Current method has been used in the aerospace and power industries to inspect cylindrical tubes and rods made from non-ferromagnetic metals. However, its applications have expanded recently and it is now being used to inspect ferromagnetic steel welds, among other new uses. This report describes the development and application of the Eddy Current method for the detection of hydrogen-assisted cracking through paint. This report will be of interest to bridge inspectors, engineers, and designers who are involved with the inspection and maintenance of our Nation's highway bridges.



T. Paul Teng, P.E.  
Director, Office of Infrastructure  
Research and Development

## NOTICE

This document is disseminated under the sponsorship of the Department of Transportation in the interest of information exchange. The United States Government assumes no liability for its content or use thereof. This report does not constitute a standard, specification, or regulation.

The United States Government does not endorse products or manufacturers. Trade and manufacturers' names appear in this report only because they are considered essential to the object of the document.

1. Report No. FHWA-RD-00-018		2. Government Accession No.		3. Recipient's Catalog No.	
4. Title and Subtitle DETECTION AND SIZING OF CRACKS IN STRUCTURAL STEEL USING THE EDDY CURRENT METHOD				5. Report Date	
				6. Performing Organization Code	
7. Author(s) Daniel Lamtenzan, Glenn Washer, and Mark Lozev, Ph.D.				8. Performing Organization Report No.	
9. Performing Organization Name and Address Nondestructive Evaluation Validation Center Federal Highway Administration 6300 Georgetown Pike McLean, VA 22101-2296				10. Work Unit No. (TRAIS)	
				11. Contract or Grant No.	
12. Sponsoring Agency Name and Address Nondestructive Evaluation Validation Center Federal Highway Administration 6300 Georgetown Pike McLean, VA 22101-2296				13. Type of Report and Period Covered  Final Report April 1996 – June 1997	
				14. Sponsoring Agency Code	
15. Supplementary Notes FHWA Contact: Glenn Washer, Program Manager, NDE Validation Center, HRDI-10 The authors would like to acknowledge the efforts of Dennis Richards, Level II technician, PSI, Inc. for his assistance in gathering the field data included in this report.					
16. Abstract  <p>This report summarizes research pertaining to the application of the Eddy Current method as a means of crack detection in structural steel members of highway bridges. Eddy currents are induced when an energized coil is placed near the surface of a conductive material. Discontinuities such as cracks disturb the trajectories of the eddy current and thus affect the magnitude and phase of the induced current. These changes can be detected by the probe. Proper probe design can eliminate the effects arising from spatial changes in material properties.</p> <p>Specimens obtained for laboratory use included a calibration block with electro-discharge machining notches with depths of 0.2, 0.5, and 1.0 mm. Five fatigue crack specimens with crack depths of 0.8, 1.0, 1.5, 2.0, and 3.0 mm were also tested. These specimens were used to evaluate voltage and frequency settings and responses. Fatigue crack profiles were successfully determined in the specimens. The effect of coatings was also tested in the laboratory using a lead-based coating and several zinc-based coatings. In general, the coatings were found to not significantly interfere with the performance of the method.</p> <p>The Eddy Current method was then used to detect cracks in the pivot girders of the Coleman Bridge over the York River in Yorktown, Virginia. These girders are protected with a zinc-based coating; therefore, other crack detection methods would have required the removal of this coating prior to testing. Eighteen indications were found in the south girder, three of which were cracks. The other 15 were distinguished from cracks by either visual inspection or signal response (for geometric indications or slag inclusions, respectively).</p> <p>Comprehensive studies on the probability of detection can be performed to determine whether or not this method can be widely implemented on steel highway bridges and to determine the reliability of the method. The Eddy Current method is a promising tool for crack detection in steel members of highway bridges.</p>					
17. Key Words Crack detection, eddy current, nondestructive evaluation, steel structures.			18. Distribution Statement No restrictions. This document is available to the public through the National Technical Information Service, Springfield, VA 22161.		
19. Security Classif. (of this report) Unclassified		20. Security Classif. (of this page) Unclassified		21. No. of Pages 26	22. Price

# TABLE OF CONTENTS

	<u>Page</u>
INTRODUCTION.....	1
FUNDAMENTALS OF THE EDDY CURRENT METHOD.....	1
INSTRUMENTATION.....	3
PROBE CHARACTERISTICS.....	4
STANDARD CALIBRATION BLOCKS AND CRACK SPECIMENS.....	5
TEST RESULTS.....	7
EDDY CURRENT IN WELD CRACK INDICATIONS.....	11
FATIGUE CRACK PROFILES.....	13
CALIBRATION CURVES.....	16
BRIDGE INSPECTION.....	17
CONCLUSION.....	22
REFERENCES.....	22

## LIST OF FIGURES

<u>Figure No.</u>	<u>Page</u>
1. Induced eddy currents for a coil with an axis parallel to the surface .....	2
2. AC bridge circuit and differential probe arrangement .....	3
3. Scanning direction of the Eddy Current method .....	4
4. Plus-point probe arrangement .....	5
5. EDM standard calibration block drawing .....	6
6. Fatigue crack specimen drawing .....	7
7. EDM notch voltage signal frequency response .....	8
8. EDM notch and fatigue crack signal frequency response .....	8
9. Effects of lead-based paint on eddy current signal.....	9
10. Effects of zinc-based paint on eddy current signal.....	10
11. Reactive and resistive components of signal response for EDM notches .....	11
12. Reactive and resistive components of the signal response for transverse-to-weld cracks .....	11
13. Longitudinal crack with probe passed along the length of the crack and centered over the flaw .....	12
14. Longitudinal in-toe crack .....	12
15. Longitudinal in-root crack.....	12
16. Fatigue crack scanning path .....	13
17. Fatigue crack profile (0.8-mm crack depth).....	14
18. Fatigue crack profile (1.0-mm crack depth).....	14
19. Fatigue crack profile (1.5-mm crack depth).....	15
20. Fatigue crack profile (2.0-mm crack depth).....	15
21. Fatigue crack profile (3.0-mm crack depth).....	16
22. Calibration curves of defect-inductive reactance signals for the EDM standard block and fatigue crack specimens.....	17
23. Signal crack indications in the south pivot girder of the Coleman Bridge.....	18
24. Output signal for a weld crack from the Zetec <sup>®</sup> plus-point probe.....	20
25. Defectometer <sup>®</sup> output signals for a weld crack.....	20

## LIST OF TABLES

<u>Table No.</u>	<u>Page</u>
1. Eddy current testing of a weld on the Coleman Bridge .....	21

## **INTRODUCTION**

Detection of cracks in steel bridges is critical to the safe maintenance of highway infrastructure. Cracks may result from welding defects that occur during fabrication or from fatigue developed during the service life of a bridge. Inadequate crack detection has led to catastrophic incidents in the past. In 1967, for example, 46 people lost their lives in the collapse of the Silver Bridge over the Ohio River at Point Pleasant, Ohio. This collapse and other less severe failures that have occurred more recently point out the need for effective crack detection methods.

Historically, the Eddy Current (EC) method has been used in the aerospace and power industries to inspect metal cylindrical tubes and rods made from non-ferromagnetic materials. However, its applications have expanded recently, and it is now being used to inspect ferromagnetic steel welds, to test objects of any shape, and to detect residual stresses. The EC method is a non-contact method that provides instantaneous test results. Its small, portable components are available at a low cost. These characteristics make the EC method appropriate for field-testing situations; however, several questions remain to be answered before it can be applied to in-service highway bridges.

This research study yielded the following results: (1) the EC method can effectively detect cracks in weld metals that have irregular surfaces and magnetic properties that vary spatially and (2) the EC method can penetrate paint coatings that are typically applied to bridges, including non-conductive coatings such as red lead paint and conductive coatings such as inorganic zinc primer. This paper reports on an actual field test of the EC method.

## **FUNDAMENTALS OF THE EDDY CURRENT METHOD**

Eddy currents are induced when an energized probe coil is placed near the surface of a conductive material. Eddy currents are proportional to the electrical conductivity of the material itself. Coil current must be AC because a time-dependent magnetic field is required to induce or generate electrical currents. As shown in figure 1, the currents induced in a metal surface oscillate in a circular pattern, flowing in a direction opposite to the current in the coil. Eddy currents induced at the surface of a test material are of a certain magnitude and phase, and vary with time. Material properties and discontinuities such as cracks disturb the trajectories of the eddy current and thus affect the magnitude and phase of the induced current. The probe senses the magnetic field induced by currents that produce a complex voltage in the coil. The EC testing method requires that the components of the potential difference across the coil or the changes in impedance be determined. Given that changes in impedance are very small, differential measurements are used to improve the resolution of the signal. Doing so involves the measurement of the differences in impedance between a pair of coils with a high-sensitivity AC Wheatstone Bridge circuit as the one shown in figure 2.

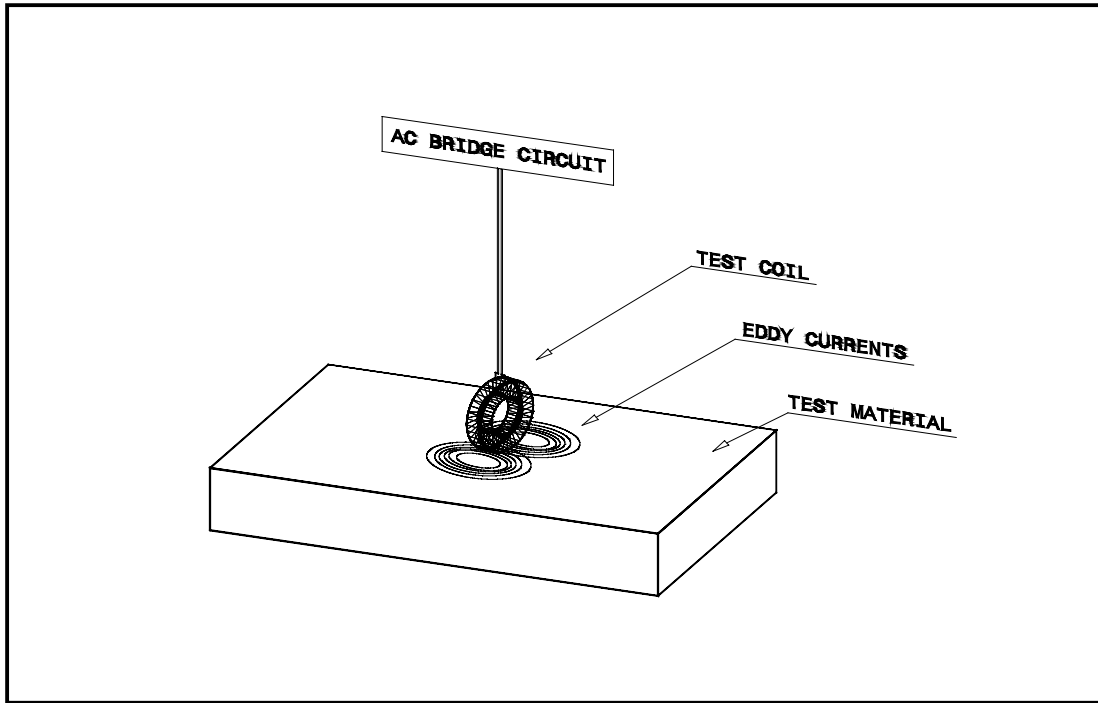


**Figure 1. Induced eddy currents for a coil with an axis parallel to the surface.**

A bridge circuit typically contains four impedance arms:  $Z_1$ ,  $Z_2$ ,  $Z_3$ , and  $Z_4$ . Balance occurs when the potential difference across the differential bridge output circuit is zero, for which:

$$\frac{Z_1}{Z_2} = \frac{Z_3}{Z_4} \quad \text{or} \quad \frac{R_1 + jX_1}{R_2 + jX_2} = \frac{R_3 + jX_3}{R_4 + jX_4} \quad (1)$$

R = Resistance

$jX$  = Inductive reactance

Impedance arms  $Z_1$  and  $Z_2$  are purely resistive and have a known and equal value. In a differential coil configuration,  $Z_3$  and  $Z_4$  are the impedance values for the probe coils. These values, which are frequency dependent, are approximately equal to each other. The input electromotive force (EMF) to the bridge is an AC oscillator that varies in frequency and amplitude. The output signal is plotted either as impedance or as a voltage plane trajectory diagram. The shape of the plane trajectory is a function of the nature of the discontinuity, and it is influenced by factors such as test material conductivity, magnetic permeability, and geometry. Some of the factors that may affect the EC test are lift-off variations, probe canting angle, and noise measurement. The two-dimensional signal, which consists of real and imaginary components of the impedance, is sampled and digitized with an analog-to-digital (A/D) converter. It is then computer-processed, and stored by a data acquisition system. Figure 3 shows the scanning direction of the EC method.

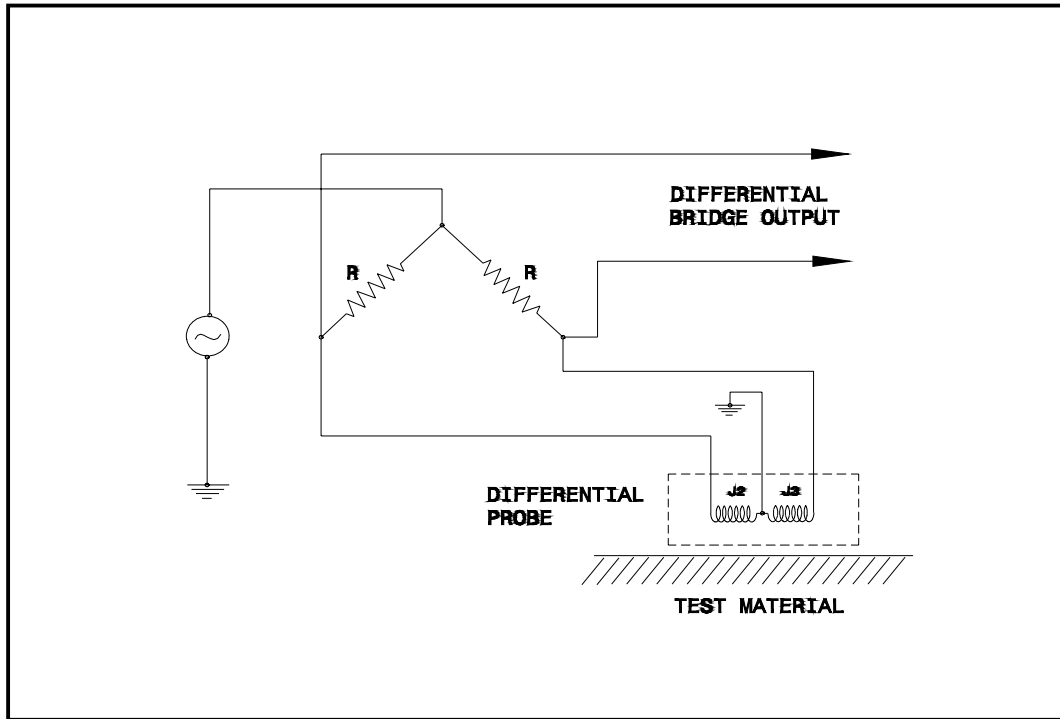


**Figure 2. AC bridge circuit and differential probe arrangement.**

## INSTRUMENTATION

Research was performed with the use of a SmartEDDY 3000 Series Instrument<sup>®</sup> that displays and stores eddy current inspection data collected by a probe. The manner in which the test signal is processed and displayed depends on the instrument settings. The values for the drive levels (voltage peak) and frequency can be selected independently from each other. The instrument voltage peak ranges from 0 to 9V, and the frequency ranges from 5 Hz to 10 MHz.<sup>(1)</sup>

Both impedance plane and voltage plane modes were used for testing. In either mode, one side of the signal source was applied to two of the bridge's arms. The first arm consists of a 50-ohm resistor connected in series with one of the coils in a differential configuration. The second arm consists of another 50-ohm resistor connected in series with the second differential coil. The difference in voltage between the two coils across the center of the bridge is amplified and passed through a demodulator that detects both in- and out-of-phase signals. These signals are then digitized to 16 bits and made available to the computer bus. In the impedance plane mode, the eddy current signal is displayed as a calibrated percentage of change in impedance. In the voltage plane mode, the signal is also generated from an impedance bridge, but the data is displayed as detected at in- and out-of-phase voltages.



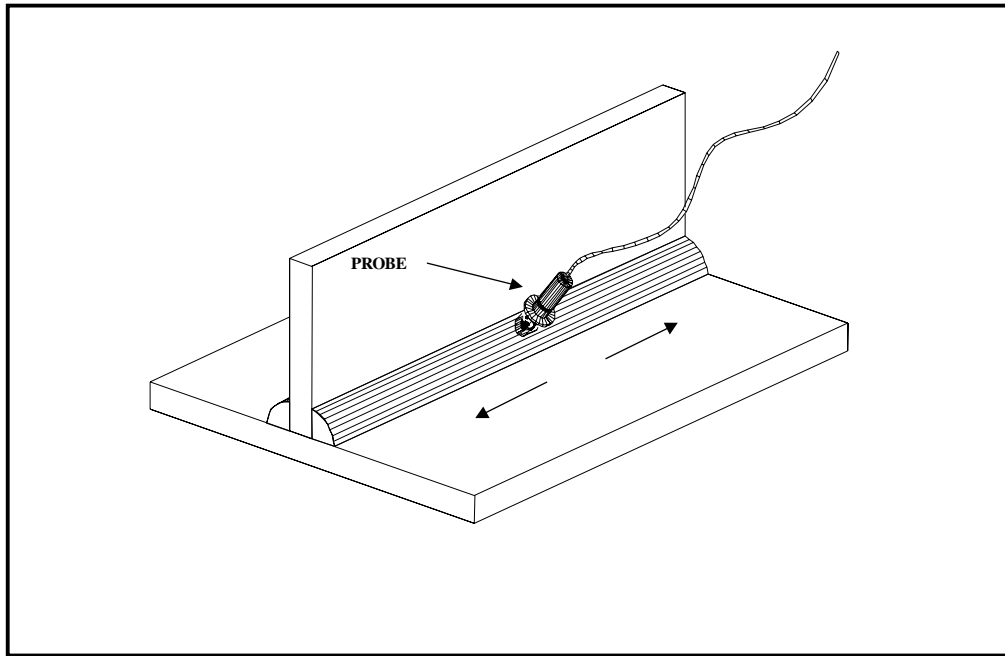


**Figure 3. Scanning direction of the Eddy Current method.**

### **PROBE CHARACTERISTICS**

A differential probe of bi-directional sensitivity was used to scan the specimens. This probe, designed by Zetec<sup>®</sup>, is capable of detecting surface-breaking cracks in plain and weld areas of steel components while minimizing changes in voltage produced by any variations in permeability or conductivity. The probe consists of two circular coils with axes parallel to the surface and perpendicular to each other. A sketch of the probe configuration is shown in figure 4. In differential configuration, a coil compares the area influenced by its own magnetic field to the area influenced by the other coil. In the event that both coils are simultaneously affected by the same material conditions, there will be no signal, meaning that the bridge is balanced. Any electromagnetic condition that is not common to the areas of the specimen being tested will produce an imbalance in the system and will be detected in the process. Since the coils are located in close proximity to each other, gradual changes caused by conductivity or permeability are limited. Lift-off effects are minimized, but not suppressed, as both coils are simultaneously affected when the distance-to-probe surface changes.

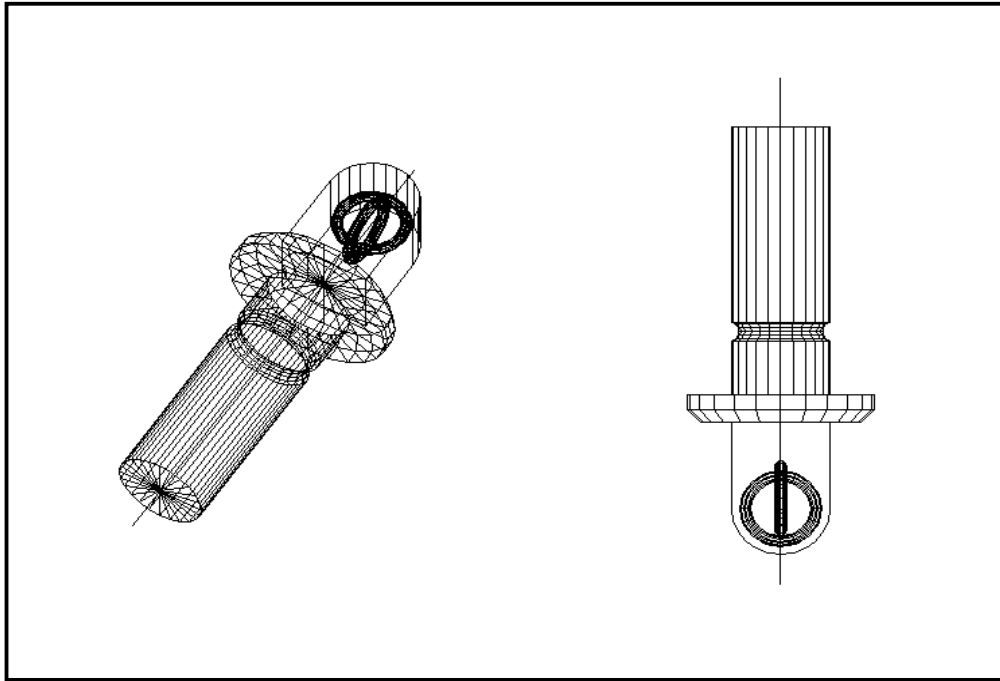


**Figure 4. Plus-point probe arrangement.**

The maximum probe response is observed when the crack is perpendicular to the direction of either winding coil. Minimal responses occur when the crack is at a  $45^\circ$  angle from the direction of the winding coil. Having approximately the same impedance, both coils are electrically connected to oppose each other. Since the two bridge arms have a resistance value of 50 ohms, the maximum sensitivity to changes in probe coil impedance occurs in coils with an impedance value of 50 ohms.<sup>(1)</sup> The probe frequency range is 100 to 800 kHz.

#### **STANDARD CALIBRATION BLOCKS AND CRACK SPECIMENS**

Three electro-discharge-machining (EDM) notches, with depths of 0.2, 0.5, and 1.0 mm ( $\pm 0.1$  mm) and a width of 0.15 mm ( $\pm 0.01$  mm), were produced in the surface of two reference standard steel specimens made from ASTM A588 (A709 Grade 50) and A36 (A709 Grade 36). These specimens were measured on an “as is” basis. That is, no attempts were made to anneal or demagnetize them. The effect of conductive coating on crack indications was studied by applying an inorganic zinc-based coating and a lead-based coating on the surface of the reference standard A588 steel specimen. The drawing of this specimen is shown in figure 5.

A second set of five fatigue crack specimens made by FlawTech, Inc. was used to study and analyze the crack-depth profile and to compare a standard EDM calibration curve with a fatigue crack-depth curve. These specimens, shown in figure 6, were made from A36 (A709 Grade 36), with depths of 0.8, 1.0, 1.5, 2.0, and 3.0 mm ( $\pm 0.25$  mm) and lengths of 20 mm.

Finally, a third set of three A588 steel specimens with surface-breaking cracks was tested. These specimens, made by Sonaspection, Inc., were welded details typical of steel bridge construction. Two of them had tee joints representing either web/stiffener or web/flange connections, and the third one contained a butt joint typically used for flange or web splices. The butt joint specimen and one of the tee specimens had complete penetration groove welds. The second tee joint was connected by a fillet weld. These specimens represented in situ cracks and were subjected to corrosive environmental conditions. Sketches of an EDM standard block and the A588 crack specimens will be shown later, together with their resulting scans.

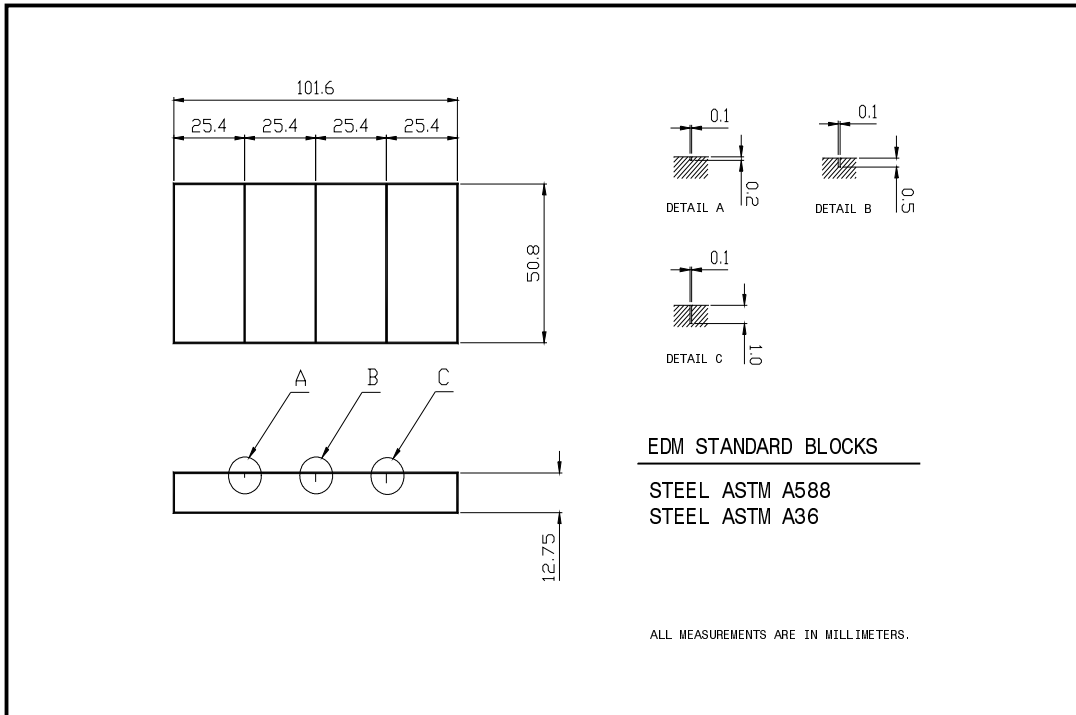


**Figure 5. EDM standard calibration block drawing.**

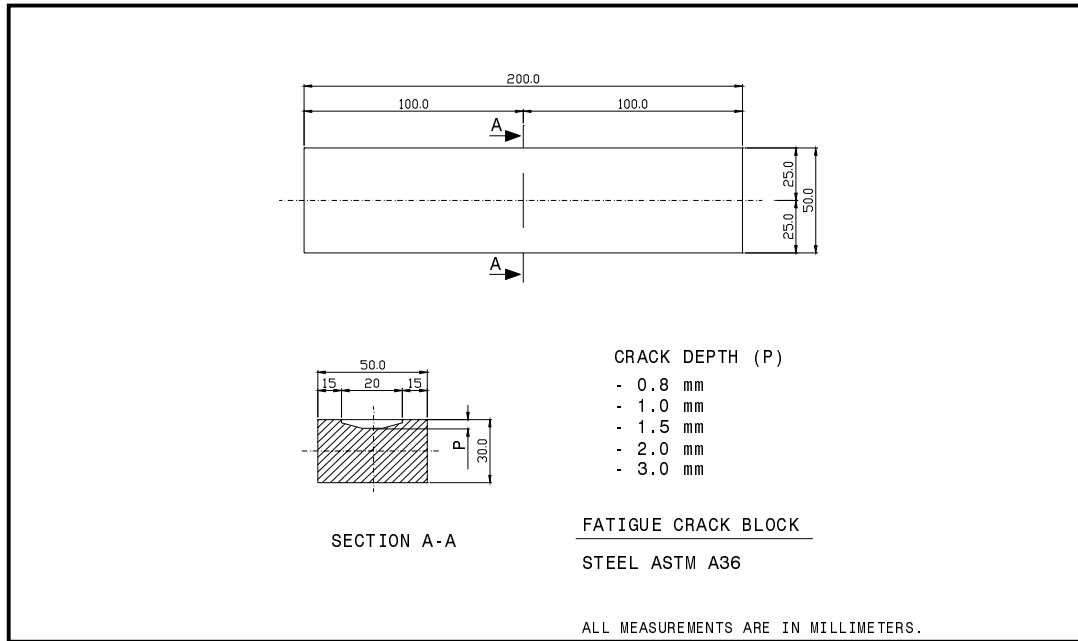


**Figure 6. Fatigue crack specimen drawing.**

## TEST RESULTS

Figures 7 and 8 represent the maximum vector magnitude of the EDM notch signals over a wide frequency range. The scanned voltage plane mode of the referenced standard A588 steel specimen is shown in figure 7. This figure indicates the variation in probe coil voltage according to the frequency of 0.2-, 0.5-, and 1.0-mm-deep EDM notches. A maximum increment in signal magnitudes for a given defect depth is observed in frequencies ranging from 200 to 300 kHz. The general shape of these curves is characteristic of bridge output sensitivity. The impedance plane mode response of two EDM notches (0.5 and 1.0 mm deep) and a 0.9-mm-deep implanted crack specimen is shown in figure 8. As expected, the variations in probe coil impedance increases along with frequency. The variation of the complex impedance signals observed in this figure's 0.5-mm-deep EDM notch is higher than the signals from the 0.9-mm-deep implanted fatigue crack. The difference in variation verifies the fact that a crack indication signal depends not only on the depth of a defect, but also on its width. Electrical contact between crack faces due to crack geometry and presence of oxides causes a short circuit of the flow of the eddy current around the crack opening and may even change the response in a considerable manner.<sup>(2)</sup> Consequently, smaller signals are expected to come from the cracks and not from the open EDM notches.

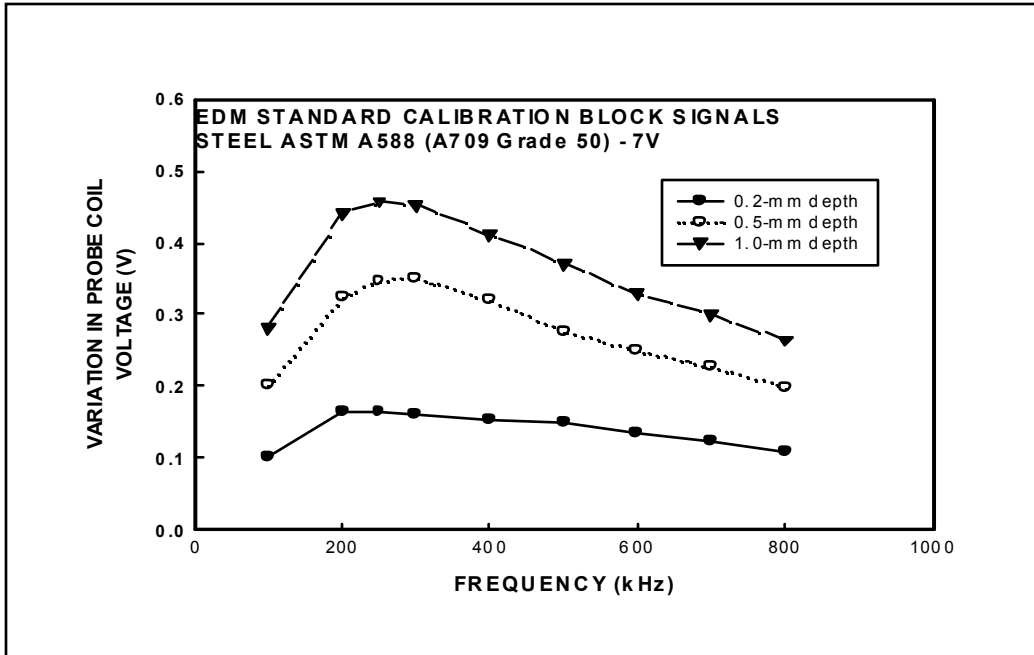


Figure 7. EDM notch voltage signal frequency response.

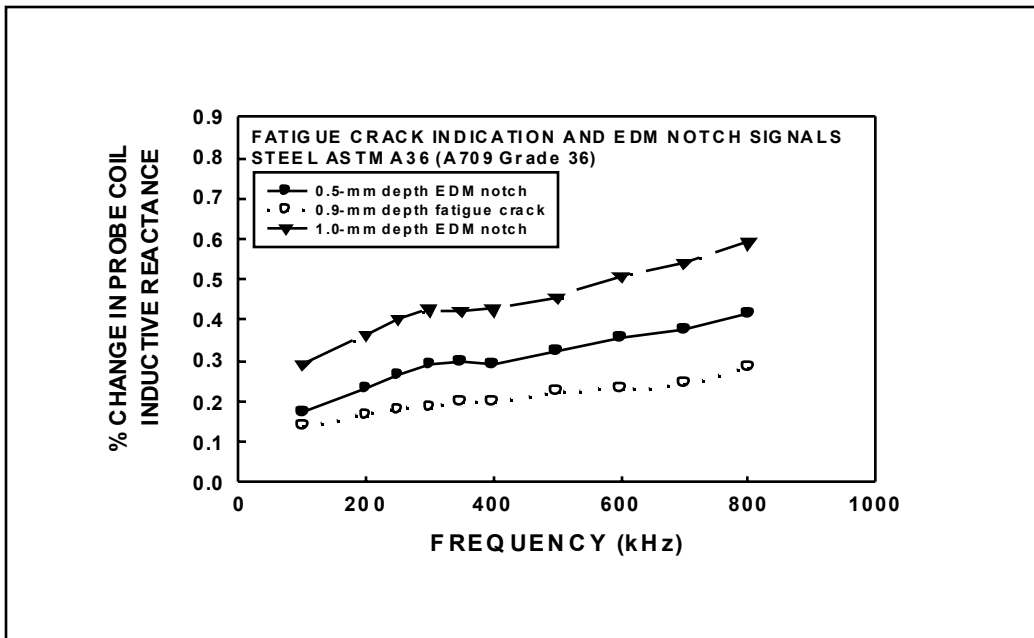


Figure 8. EDM notch and fatigue crack signal frequency response.

The effect of typical coatings on eddy current signals is shown in figures 9 and 10. Both figures show the variation in the complex impedance components according to the frequency of a 1.0-mm EDM notch that is neither covered by zinc- or red lead-based coatings. In these figures, a progressive attenuation of the inductive reactance amplitude is observed due to the lift-off effect and distribution of the eddy currents within the coating layer. This attenuation is proportional to the coating thickness. The low electrical conductivity of the coating layer ensures the penetration of the eddy currents into the base metal. In fact, no significant variations are observed between signals affected by the 0.4-mm red lead-based coating or the 0.4-mm lift-off. Similar results can be observed with the zinc-based system.

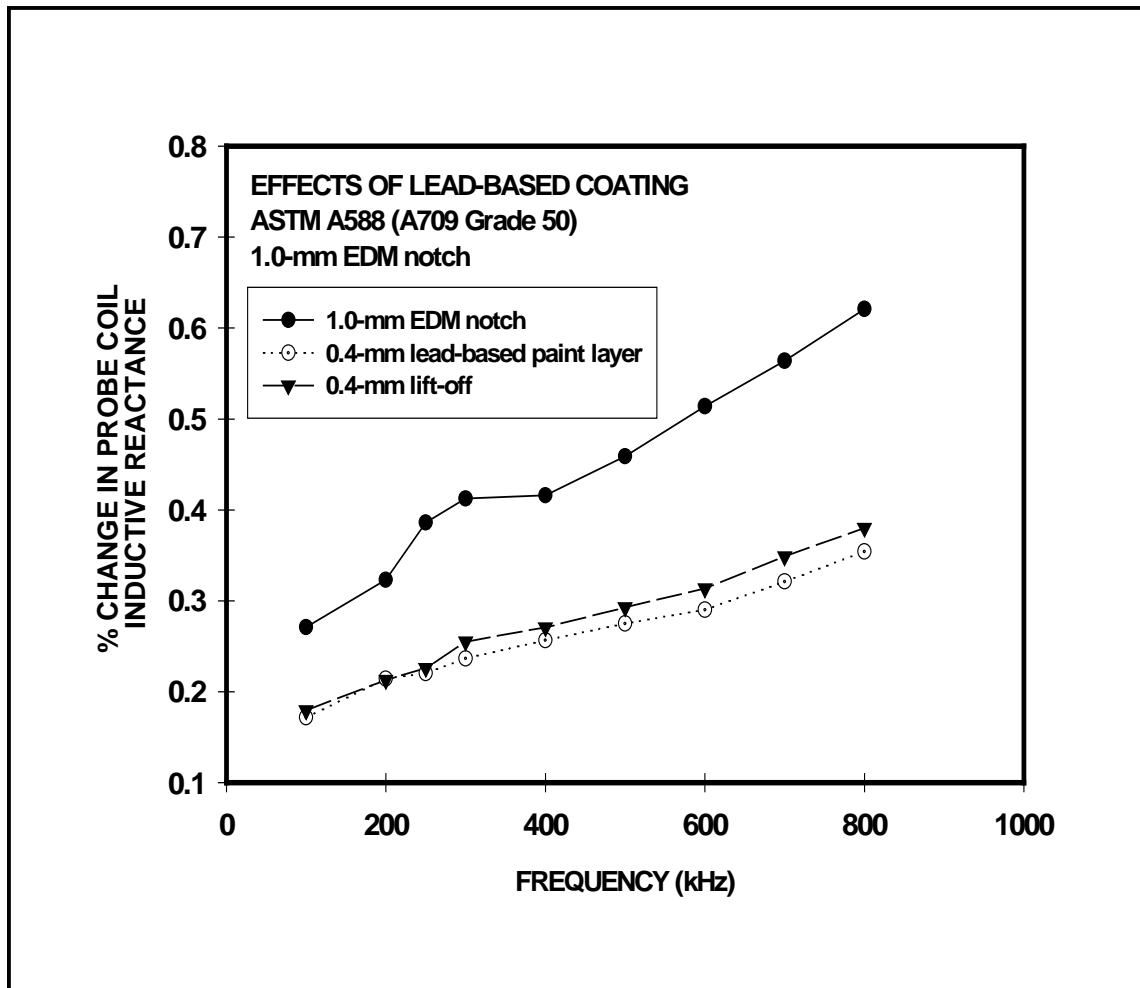
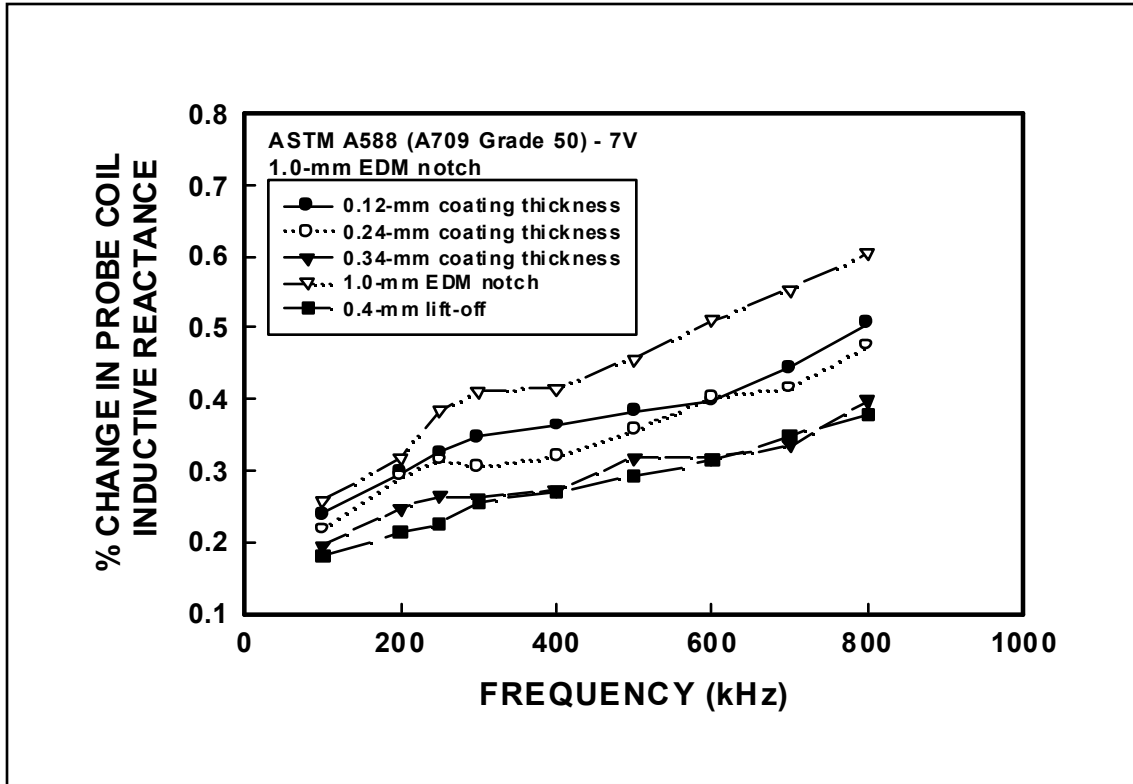


Figure 9. Effects of lead-based paint on eddy current signal.



**Figure 10. Effects of zinc-based paint on eddy current signal.**

Figures 11 through 15 show the percentage change in probe coil inductive reactance of the impedance components according to probe displacement. The frequency and drive level at which the EDM notches and fatigue cracks were scanned were 240 kHz and 3V, respectively. At this frequency, the probe impedance is essentially reactive, and its signal-to-noise ratio is acceptable. The resistive component of the impedance was observed to be a simple, increasing function of frequency, which is relatively insensitive to changes in test conditions. Due to the relatively high magnetic permeability of the specimens, the eddy currents concentrate within very shallow layers of the near-surface regions. A penetration depth of approximately 0.12 mm at 240 kHz was observed for the standard A588 steel specimen. This value is not an indicator of the maximum crack depth that can be detected by a probe, yet it still affects probe resolution and signal-to-noise ratio. The induced eddy currents will follow the crack contour and, as a result, the crack's shape, orientation, and thickness determine the manner in which impedance will change as the probe moves across it.

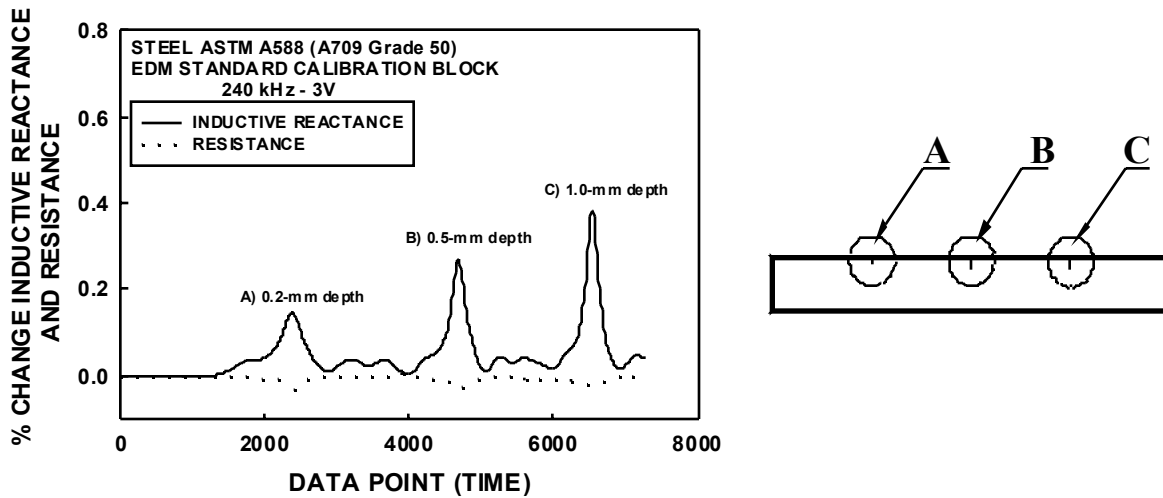


Figure 11. Reactive and resistive components of signal response for EDM notches.

### EDDY CURRENT IN WELD CRACK INDICATIONS

The following figures are examples of eddy current crack indications for different types of joints and crack positions. The eddy current signals of crack indications are strongly affected by the weld joint finish, which is one of the most important noise sources that has not yet been suppressed by any differential probe. Weld discontinuities such as porosity, slag inclusions, undercuts, and rollovers are usually found in zones adjacent to the weld and on the weld crown. These discontinuities can create false crack indications, especially when trying to detect small cracks ( $\leq 0.2$  mm).

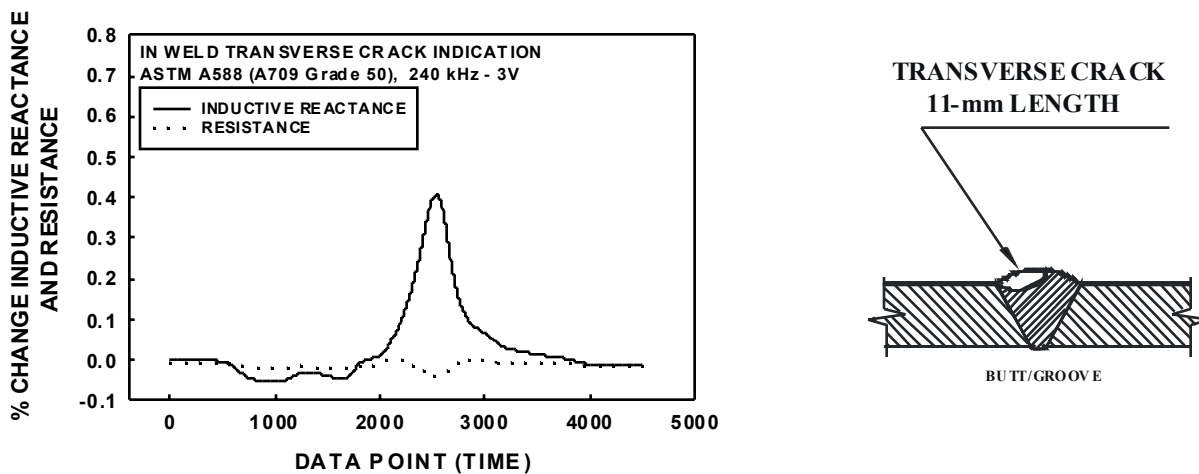


Figure 12. Reactive and resistive components of the signal response for transverse-to-weld cracks.



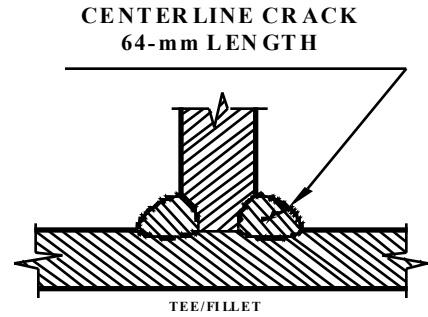
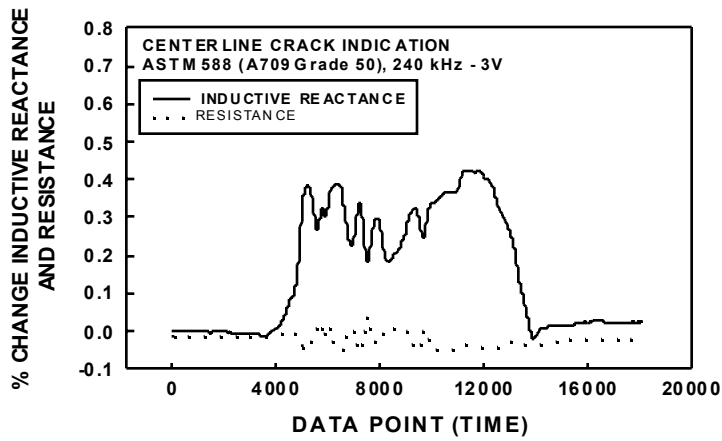


Figure 13. Longitudinal crack with probe passed along the length of the crack and centered over the flaw.

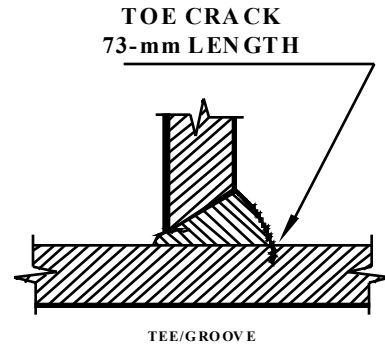
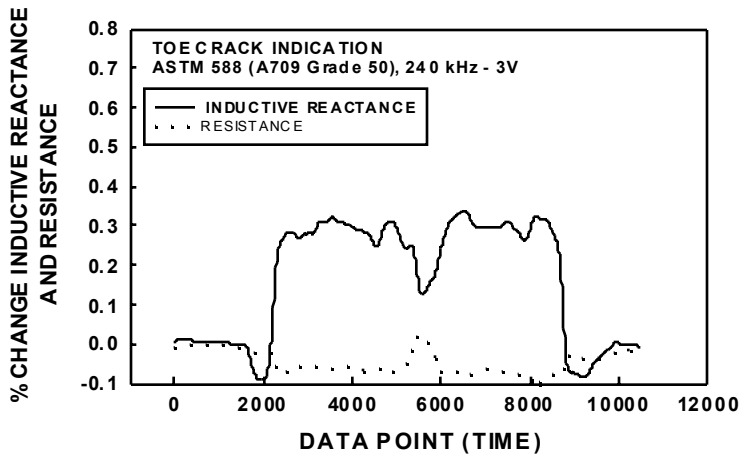


Figure 14. Longitudinal in-toe crack.

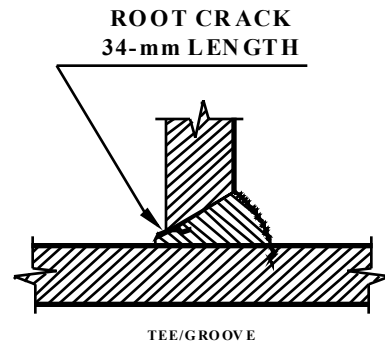
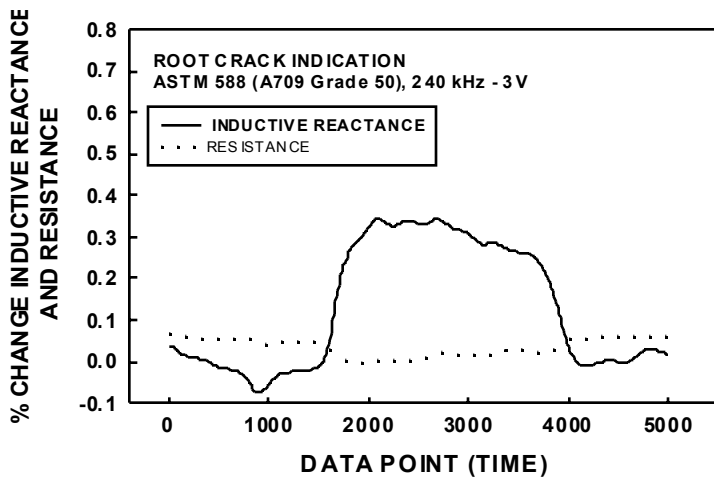
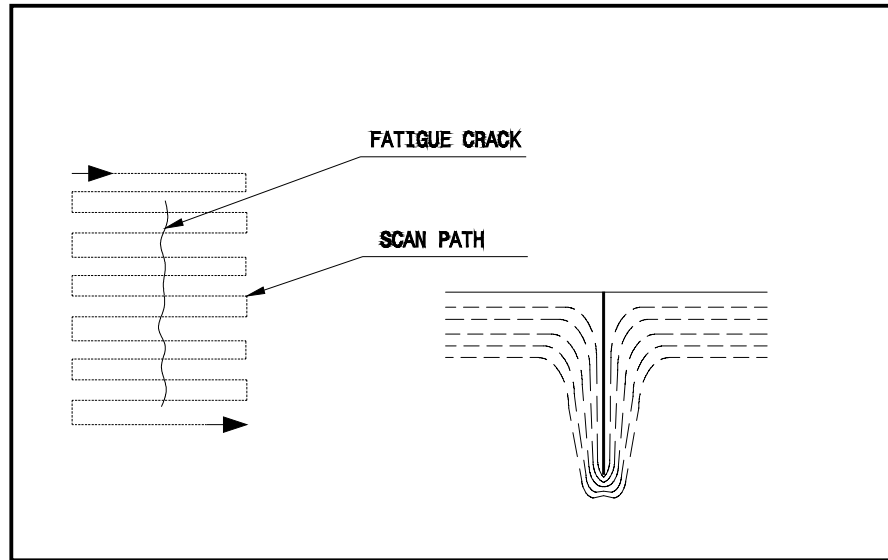


Figure 15. Longitudinal in-root crack.

## FATIGUE CRACK PROFILES

Traditionally, the EC method has only been used to obtain qualitative characteristics that detect and indicate the presence or absence of a flaw. However, quantitative data also contain important information regarding a flaw's shape and size. The procedure described in this section was performed with the goal of obtaining fatigue profiles for the specimens in this study. Data were collected as the probe moved transversally across the length of the flaws.



**Figure 16. Fatigue crack scanning path.**

Given the “as is” condition of the material, it was expected for residual magnetization, electric conductivity, and variations in magnetic permeability to appear on the specimens. Magnetic permeability is one of the most important parameters to consider when working with magnetic materials. It indicates how much magnetic induction is being generated from a material in a given magnetic field. However, it is deeply affected by residual magnetic fields and the history of the material itself. In general, ferromagnetic materials present no constant values for permeability. When specimens are being manufactured, changes in material microstructure may appear in the form of additional magnetic inclusions. The development of particles with different magnetic properties, for example, may cause changes in the hysteresis properties of the material. In addition, plastic deformation and cold working conditions may increase the number of density dislocations in terms of tension or compression, which affect the values for permeability.<sup>(3)</sup>

Four scans were performed on the crack surfaces to attenuate the noises observed with the variations in magnetic permeability (see figure 16). The data set collected was arranged to overlap the maximum points of the four scan signal indications. Crack profiles were then estimated by calculating the mean of the data samples. Figures 17 through 21 show the fatigue

crack profiles for the specimens. Given that the EC test results occur repetitively, the distribution of the data points used to fit the crack profile is quite consistent throughout these figures. The percentage change in inductive reactance signal increases along with the depth of the defect.

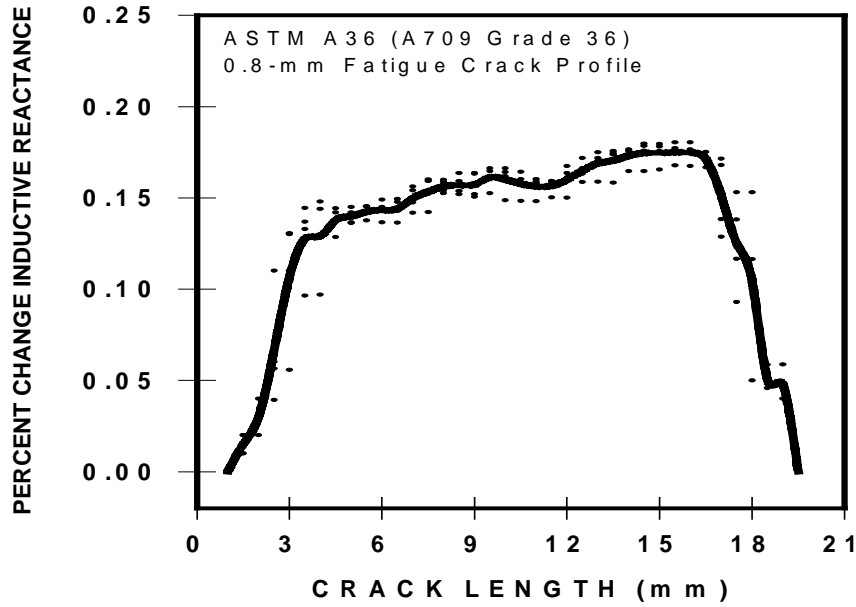


Figure 17. Fatigue crack profile (0.8-mm crack depth).

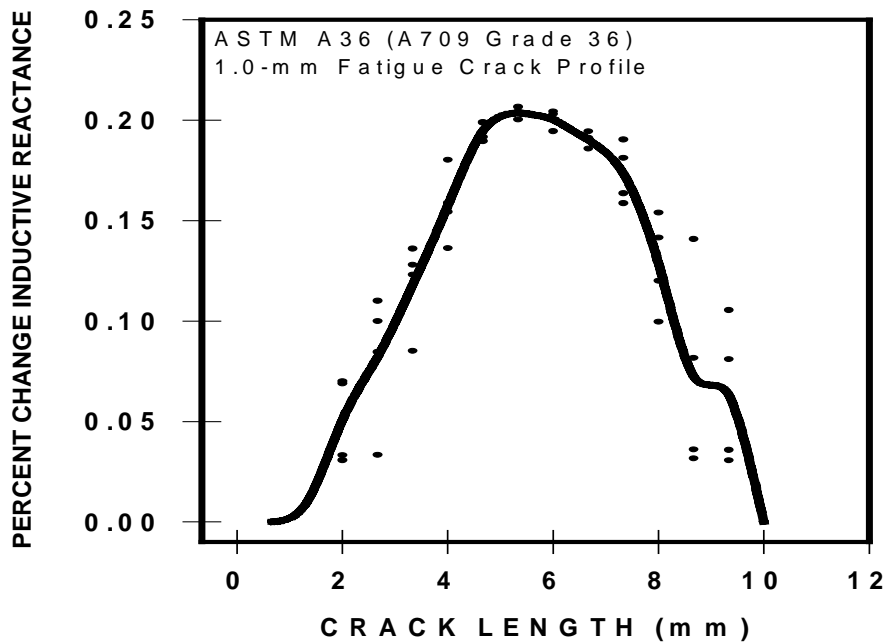


Figure 18. Fatigue crack profile (1.0-mm crack depth).

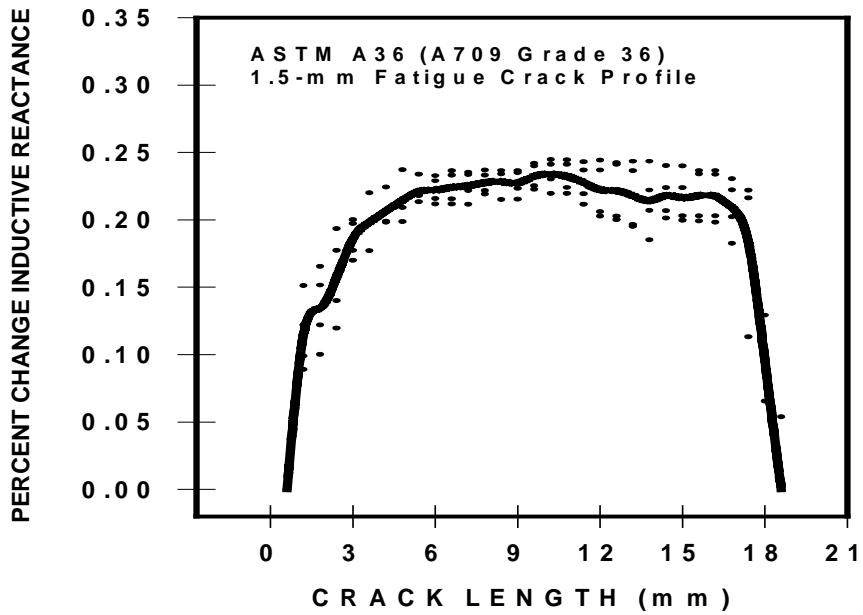


Figure 19. Fatigue crack profile (1.5-mm crack depth).

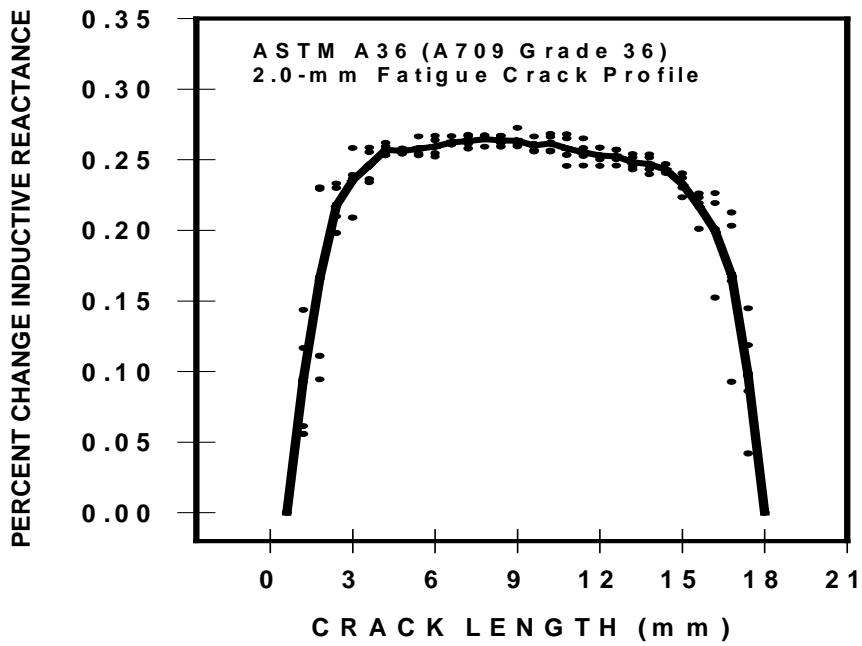


Figure 20. Fatigue crack profile (2.0-mm crack depth).

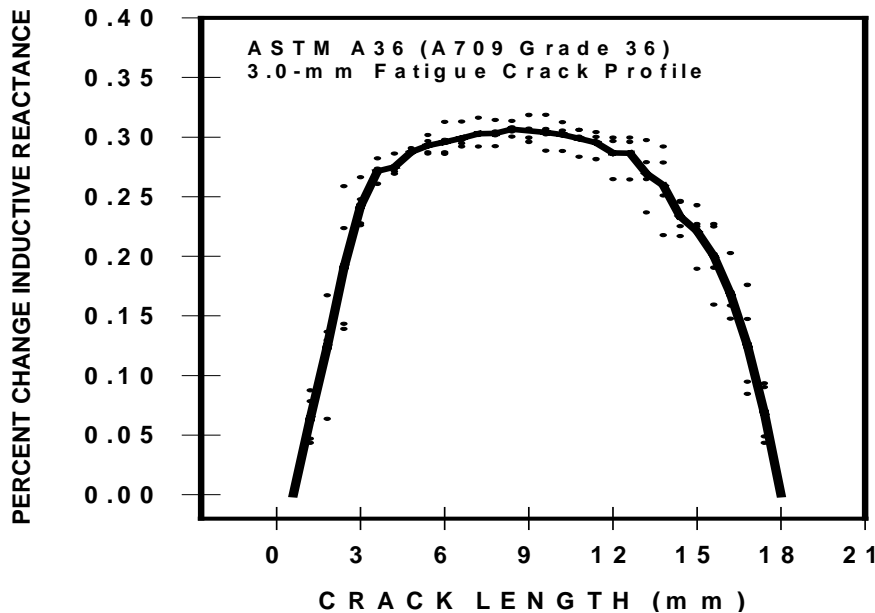


Figure 21. Fatigue crack profile (3.0-mm crack depth).

## CALIBRATION CURVES

Important factors must be taken into account when calibration reference standards are used to verify the accuracy of electromagnetic testing. Reference standards must simulate the actual parts that are being inspected. The physical, electrical, and magnetic characteristics of the test material must be duplicated according to them. Variables to be controlled and taken into account during fabrication include geometry, conductivity, permeability, surface finish, and coating.

Given that the shape and size of a notch can be accurately controlled during the fabrication process, longitudinal EDM notches are the first choice when it comes to the production of reference standards. It is possible to produce notches of widths as small as 0.10 mm, with a degree of tolerance on the order of  $\pm 0.01$  mm. On the other hand, fatigue crack specimens can also be used as reference standards. The obvious advantage of this technique over others is that it can closely simulate real discontinuity, even though this occurs at the expense of acquiring specimens and producing accurate crack dimensions. The maximum fatigue crack depth that can be produced is 4.0 mm, with a tolerance range of  $\pm 0.25$  mm.

Other factors to be considered are the geometry and orientation of the crack within the material. The magnitude of output signal is strongly affected by crack orientation. The maximum value of a signal can only be obtained when the vertical depth of the crack tip lies below the surface. It is common for calibration reference standards to have perpendicular-to-surface defects.

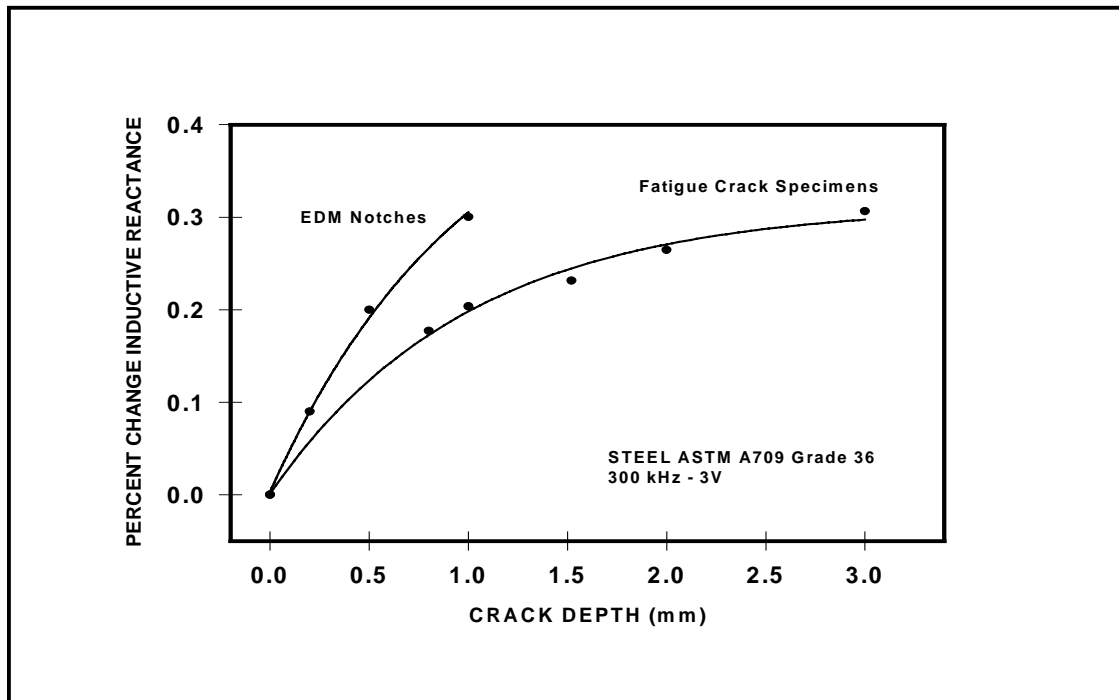


**Figure 22. Calibration curves of defect-inductive reactance signals for the EDM standard block and fatigue crack specimens.**

The signal response from an EDM notch is not the same as that from a fatigue crack. Figure 22 shows the calibration curve of defect-inductive reactance signals with increasing defect depths for the ASTM A709 (Grade 36) EDM standard block and the fatigue crack specimens. Both the EDM standard calibration block and the fatigue crack specimens are made up of the same material and have vertical-to-surface defects of different depths. These curves can only be used at a given frequency and input voltage value. The test frequency and drive levels were set to 300 kHz and 3V. Signals coming from the EDM standard block present higher percentage change values in inductive reactance than the ones coming from the fatigue crack specimens. This result is probably due to differences in the gap between the faces of the EDM notches and the fatigue crack.

## **BRIDGE INSPECTION**

The Eddy Current (EC) method was field tested in the pivot girders of the Coleman Bridge over the York River in Yorktown, Virginia, where a fracture critical member supported the south span of a swing bridge. The pivot girder supporting the north span of the bridge presented time-delayed hydrogen cracking following production and shipping to the bridge site. Magnetic particle inspection (MPI) had revealed a total of more than 150 cracks in this member during inspections performed at the fabrication plant and after shipment and installation at the bridge site. The MPI procedure required removal of a zinc-based coating to facilitate contact between the prods and the member. But given that this procedure was undesirable to the bridge owner, the

EC method was used instead to perform an inspection of the south girder. Both pivot girders were in place on the structure at the time of the inspection.

The member inspected was constructed from A709 Grade 70W steel, with multi-pass fillet welds located on the intersection of each corner of the box and along the stiffeners. The plate thickness ranged from 32 mm to 76 mm. The zinc-based coating on the structure was approximately 0.20 mm thick, based on measurements taken on the north girder. The coating system included both an intermediate layer and a finish layer, totaling approximately 0.4 mm to 0.5 mm in thickness. The surface scanning of approximately 250 m of fillet weld included all flange/web and web/stiffener welds. Inspection of the weld bead required between three and five passes of the probe for complete coverage of both the weld surface and the heat-affected zone.

The fatigue cracks detected by the MPI on the north girder were used as test specimens to determine the appropriate frequency and drive levels for the probe. A calibration specimen was made from a piece of A709 steel containing EDM notches with depths of 0.5, 1.0, and 2.0 mm. Lift-off due to coating was assumed to reduce signal amplitudes by approximately 40 percent, thus compensating for the calibration procedure. Indications were determined by a simple reactance threshold, equivalent to approximately 20 percent of the full screen height. Any signals exceeding this threshold level were considered to be signal crack indications.

Figure 23 shows the signal crack indications found on the south girder. Table 1 describes the position, location in the weld, and direction of the crack indications that were excavated with a mechanical grinder to confirm their source in the weld. Of the 18 existing indications, 3 of them correlated with cracks. The remaining balance could be distinguished from the cracks by visual inspection in the case of geometric indications and by signal response in the case of slag inclusions.

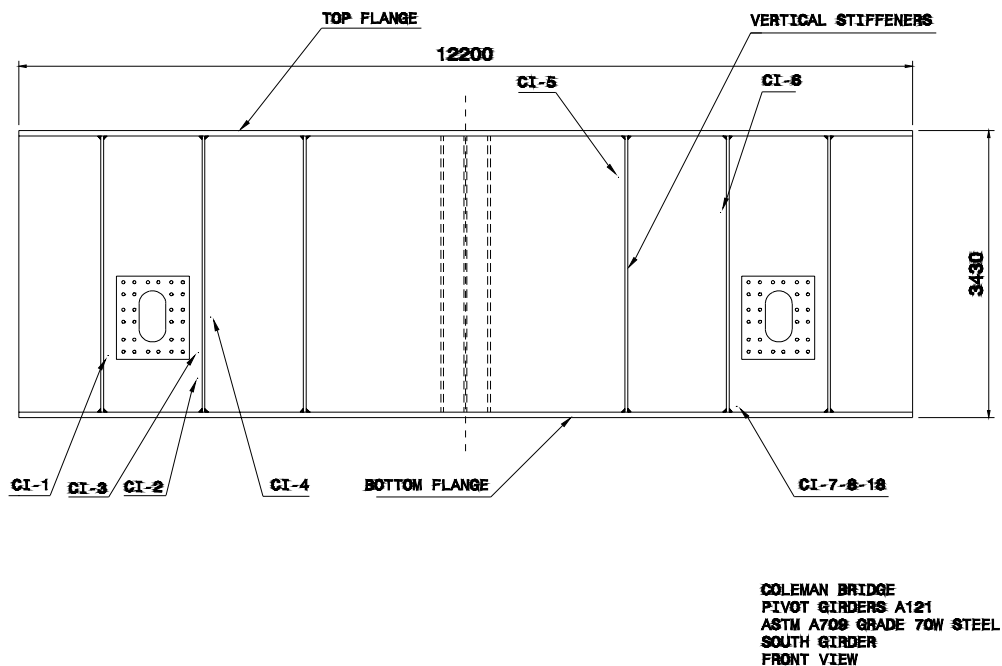
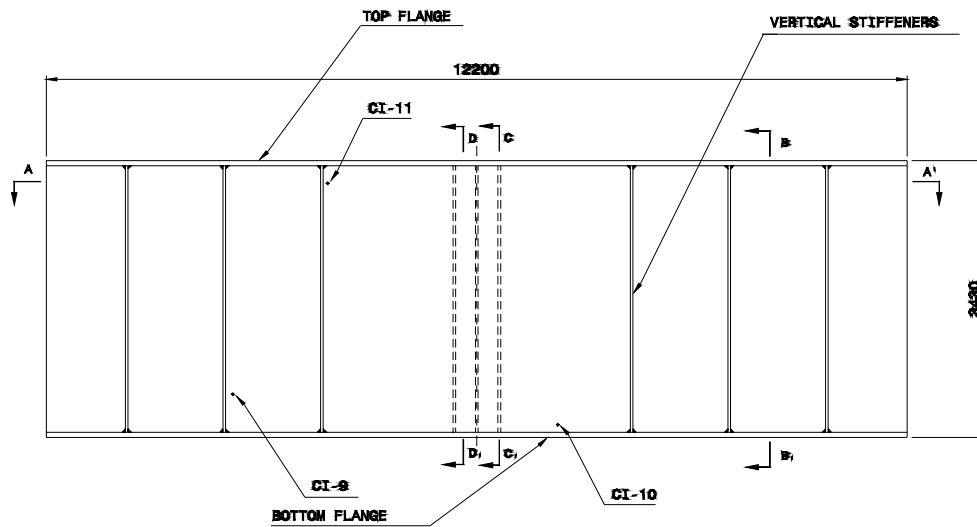


**Figure 23. Signal crack indications in the south pivot girder of the Coleman Bridge.**



COLEMAN BRIDGE  
 PIVOT GIRDERS A121  
 ASTM A709 GRADE 70W STEEL  
 SOUTH GIRDER  
 BACK VIEW

**Figure 23. Signal crack indications in the south pivot girder of the Coleman Bridge (continued).**

Due to the time-dependent nature of the cracking in the north girder, periodic inspections of the girder were scheduled every 3 months. Selection of the EC method for these inspections was not only based on the fact that the method was fast and easy to apply, but also because of the success with which cracks had been located in the south girder without the need for removal of paint coatings. The instrument used in these inspections was the Förster Defectometer<sup>®</sup>, a portable, battery-operated EC instrument. This instrument uses a 4-MHz absolute probe with a footprint much smaller than that of the Zetec<sup>®</sup> plus-point probe. Unlike the footprints of other probes, this one has the capability of reducing sensitivity to geometric indications. The Förster Defectometer<sup>®</sup> is self-balancing and displays indications as normalized impedance.

Figures 24 and 25 compare the results of the Zetec<sup>®</sup> plus-point probe, operated at 850 kHz, with those of the Förster Defectometer<sup>®</sup> for the same crack. As shown, both probes are capable of detecting the same crack and yielding similar results. Figure 24 indicates the response from the Zetec<sup>®</sup> plus-point probe, showing a percent change in inductive reactance as the probe is scanned over a transverse crack. The resistive component of the signal is insignificant. The Förster Defectometer<sup>®</sup> indicates the normalized impedance value for the same transverse crack.



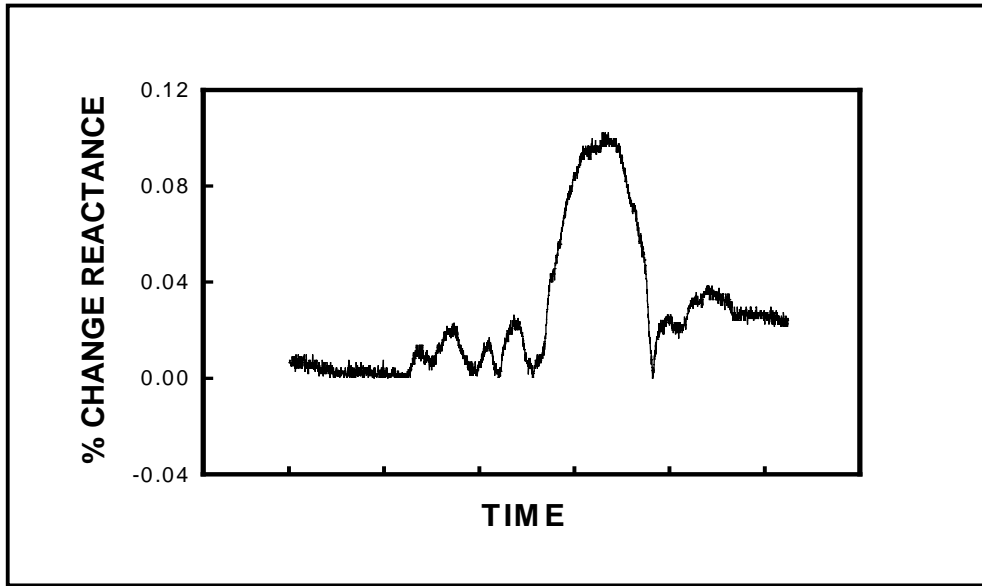


Figure 24. Output signal for a weld crack from the Zetec® plus-point probe.

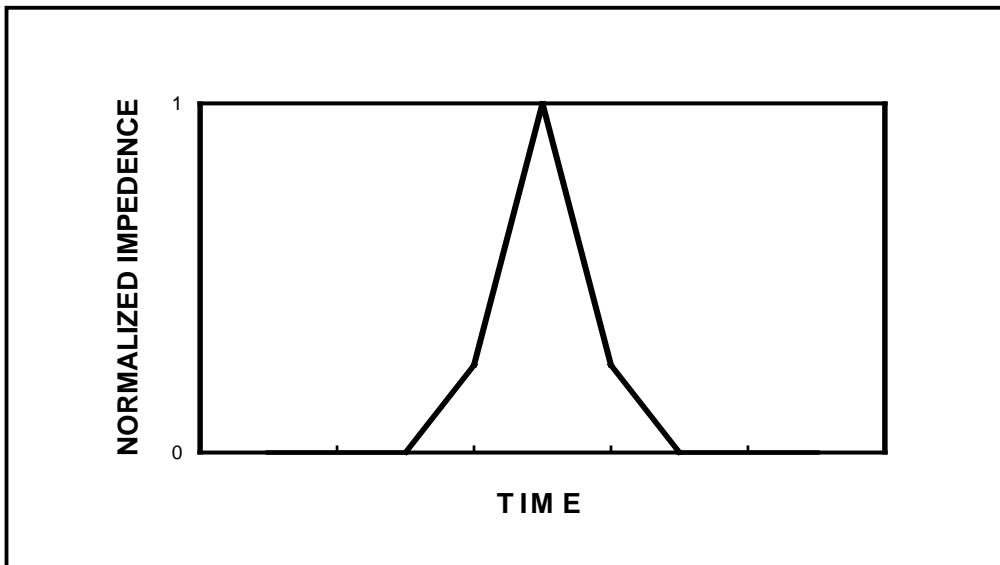


Figure 25. Defectometer® output signals for a weld crack.

**Table 1. Eddy current testing of a weld on the Coleman Bridge.**

<b>CRACK INDICATION (CI) NUMBER</b>	<b>DIRECTION OF CI</b>	<b>CI LOCATION IN WELD</b>	<b>POSITION OF CI ON SOUTH GIRDER</b>
1	Longitudinal	Toe	In S-1 to north web weld, 3251 mm down from top flange.
2	Longitudinal	Toe	In S-2 to north web weld, 654 mm up from bottom flange.
3	Longitudinal	Toe	In S-2 to north web weld, 990 mm up from bottom flange.
4	Longitudinal	Toe	In S-2 to north web weld, 1270 mm down from top flange.
5	Longitudinal	Toe	In S-7 to north web weld, 419 mm down from top flange.
6	Longitudinal	Toe	In S-8 to north web weld, 978 mm down from top flange.
7	Longitudinal	Toe	In S-8 to bottom web flange, 241 mm out from north web.
8	Longitudinal	Toe	In S-8 to bottom weld flange, 152 mm out from north web.
9	Longitudinal	Toe	In S-8 to bottom flange weld, 140 mm out from north web.
10	Transverse	Crown	In S-8 to south web weld, 140 mm up from bottom flange.
11	Longitudinal	In web	In south web between S-7 and S-3, 13 mm down from top flange.
12	Longitudinal	Toe	In S-7 to south web weld, 89 mm down from top flange.
13	Longitudinal	Toe	In bottom flange to north web weld, between B-1 and B2, 267 mm from B-2.
14	Longitudinal	Toe	In B-2 to north web weld, 883 mm down from top flange.
15	Longitudinal	Toe	In B-3 to bottom flange weld, 476 mm in from north web.
16	Longitudinal	Toe	In B-4 to south web weld, 1499 mm up from bottom flange.
17	Longitudinal	Toe	In B-4 to south web weld, 2006 mm up from bottom flange.
18	Longitudinal	Crown	In B-5 to south web weld, 152 mm up from bottom flange.

S = Stiffener  
 B = Diaphragm

## CONCLUSION

The laboratory test results indicate that a plus-point probe configuration can be used to detect cracks in weld metal. The effects of spatially varying magnetic properties can be essentially suppressed by the probe coil design. When scanning the weld bead, primary noise sources result from variations in material conductivity, permeability, and geometric effects. Laboratory tests have also shown that eddy currents can penetrate both conductive and non-conductive coatings typically used on bridges. Coating effects, which are similar to lift-off effects, are proportional to the thickness of the coating. The attenuation caused by these effects can result in increased sensitivity to geometric indications that may, in turn, mask smaller defects.

The existing relationship between probe coil response and crack depth for the plus-point probe used on ferromagnetic materials has been studied. Laboratory results indicate that EDM notches have higher electromagnetic responses than fatigue cracks due to differences in defect width. The electrical contact between crack faces causes a short circuit of the flow of the eddy currents around the crack opening. Additional research must be performed in order to define the existing relationship between calibration curves from manufactured fatigue cracks and in situ fatigue cracks. Such relationship may be studied through the use of different non-destructive evaluation (NDE) techniques that characterize flaws and compare test results. Comprehensive studies on the probability of detection must be performed to determine whether or not this method can be widely implemented on steel highway bridges.

The differential plus-point probe performed well under the field conditions of this research. Probe response to field variables such as conductive coating thickness, irregular weld surfaces, and weld joint geometry was acceptable. The EC method was proven to have the following advantages in field applications over techniques such as MPI: (1) there is no need for coating removal to ensure good prod contact, (2) utilization of the plus-point probe is effective for detection of both longitudinal and transverse cracks in weld metal, and (3) crack detection can be accomplished with high-frequency absolute coils.

It is our recommendation that bridge inspections be performed by properly qualified individuals and that optimal probe frequency be determined with a probe coil frequency test prior to any inspection. Interpretation of the eddy current signals can be accomplished with a moderate amount of training and experience.

## REFERENCES

1. *SmartEDDY<sup>®</sup> 3.0 Test Software User Guide, Version 3.3021*. SE Systems, Inc., 1995.
2. *Nondestructive Testing Handbook, Vol. 4: Electromagnetic Testing*, Second edition. American Society for Nondestructive Testing, London, 1986.
3. Jiles, David. *Introduction to Magnetism and Magnetic Materials*, First edition. Chapman & Hall, London, 1991.